MNRAS **000**, 000–000 (0000) Preprint 6 May 2025 Compiled using MNRAS LATEX style file v3.0

Baryon Acoustic Oscillations from a Different Angle

George Efstathiou
Kavli Institute for Cosmology Cambridge and Institute of Astronomy, Madingley Road, Cambridge, CB3 OHA.

6 May 2025

arXiv:2505.02658v1 [astro-ph.CO] 5 May 2025

ABSTRACT
This paper presents an alternative way of analysing Baryon Acoustic Oscillation (BAO) distance measurements via rotations to define new quantities $\mathcal{D}^{\rm perp}$ and $\mathcal{D}^{\rm par}$. These quantities allow simple tests of consistency with the *Planck* ΛCDM cosmology. The parameter $\mathcal{D}^{\rm perp}$ is determined with negligible uncertainty from *Planck* under the assumption of ΛCDM. Comparing with measurements from the Dark Energy Spectroscopic Instrument (DESI), we find that the measurements of $\mathcal{D}^{\rm perp}$ from Data Release 2 (DR2) move into significantly better agreement with the *Planck* ΛCDM cosmology compared to DESI Data Release 1 (DR1). The quantity in the orthogonal direction $\mathcal{D}^{\rm par}$ provides a measure of the physical matter density ω_m in the ΛCDM cosmology. The DR2 measurements of $\mathcal{D}^{\rm par}$ also come into better agreement with *Planck* ΛCDM compared to the earlier DR1 results. From the comparison of *Planck* and DESI BAO measurements, we find no significant evidence in support of evolving dark energy. We also investigate a rotation in the theory space of the w_0 and w_a parameterization of the dark energy equation-of-state $w(z)$. We show that the combination of DESI BAO measurements and the CMB constrain $w(z=0.5) = -0.996 \pm 0.046$, i.e. very close to the value expected for a cosmological constant. We present a critique of the statistical methodology employed by the DESI collaboration and argue that it gives a misleading impression of the evidence in favour of evolving dark energy. An Appendix shows that the cosmological parameters determined from the Dark Energy Survey 5 Year supernova sample are in tension with those from DESI DR2 and parameters determined by *Planck*.

Key words: cosmology: cosmological parameters, dark energy, supernovae

1 INTRODUCTION

Baryon acoustic oscillation (BAO) features in the galaxy distribution have provided a powerful geometrical test of the background expansion history of the Universe since they were first detected (Cole et al. (2005); Eisenstein et al. (2005), for a review see Weinberg et al. (2013)). BAO measurements have played a critical role in the development of the ΛCDM cosmology in the intervening 20 years and have become more accurate as galaxy surveys have increased in size. In addition, the redshift reach has increased to beyond $z = 2$ through measurements of BAO features in the distribution of quasars and quasar Lyα absorption lines. BAO are complementary to observations of anisotropies in the cosmic microwave background radiation (CMB). In particular, BAO measurements break geometrical parameter degeneracies in extensions of the ΛCDM cosmology which include spatial curvature and evolving dark energy. The analysis presented in Planck Collaboration et al. (2020) combined *Planck* CMB data with BAO results from the completed Sloan Digital Sky Survey Baryon Oscillation Spectroscopy Survey (BOSS) (Alam et al. 2017) finding consistency with the base 6-parameter ΛCDM cosmology, with no evidence for spatial curvature or evolution in the equation-of-state of dark energy.

However, BAO measurements from the first year of observations with the Dark Energy Spectroscopic Instrument (DESI) have, it is claimed, provided intriguing indications of evolving dark energy (EvDE[1])(DESI Collaboration et al. 2024). These hints are still present in the three year DESI BAO results (DESI Collaboration et al. 2025). Henceforth we will refer to the these two DESI papers as DESI-DR1 and DESI-DR2. The question of whether the evidence for EvDE from BAO has *strengthened* between DR1 and DR2 is addressed in this paper.

The existence of dark energy poses a fundamental problem in physics and remains unexplained (see e.g. the review by Weinberg 1989). A discovery of EvDE would have profound implications for physics and could perhaps provide a

[1] We use the acronym EvDE for evolving dark energy, to avoid confusion with the acronym EDE for early dark energy. For a review of EDE see e.g. Poulin et al. (2023).

© 0000 The Authors

path towards a theoretical understanding the origin of dark energy. It should therefore come as no surprise that the DESI results have spawned a huge number of papers, some geared towards phenomenological models of dark energy, which will not be discussed here, and some devoted to the interpretation of the DESI results, which is the focus of this paper.

We will first briefly review the main DESI results using numbers from DESI-DR2. The DESI team claim that the BAO measurements are in tension with the base ΛCDM cosmology preferred by *Planck* at the 2.3σ level (implying odds against DESI and *Planck* being compatible at about $50:1$). If the equation-of-state with redshift z is parameterised as

$$w(z) = w_0 + w_a \left(\frac{z}{1+z}\right), \tag{1}$$

(Chevallier & Polarski 2001; Linder 2003), EvDE is preferred over *Planck* ΛCDM at the 3.1σ level if DESI BAO are combined with *Planck* CMB measurements. Furthermore, if constraints from the magnitude redshift relation of Type Ia supernovae (SN) are included, the preference for EvDE lies between $2.8-4.2\sigma$ depending on the choice of SN sample. The impression given by the DESI collaboration is that each time additional data, such as the CMB and SN are added to the analysis, including the improvements in the BAO measurements from DR1 to DR2, the evidence for EvDE *strengthens*. Needless to say, such a potentially important result has attracted a huge degree of interest and generated a diverse range of views [2].

The purpose of this paper is to investigate whether the evidence for EvDE has actually strengthened between DESI-DR1 and DESI-DR2. We first note that the high significance levels [3] in favour of EvDE come from combining DESI BAO data with the DES5Y SN sample (Sánchez et al. 2024; Vincenzi et al. 2024; DES Collaboration et al. 2024). In contrast, the Pantheon+ sample of Scolnic et al. (2022) is neutral to EvDE. The Union3 compilation of Rubin et al. (2023) lies somewhere in between Pantheon+ and DES5Y. Thus different SN samples, which contain a high degree of overlap with each other, give different results. In a previous paper, I showed that inferences on EvDE from SN catalogues are very sensitive to the photometric accuracy of the SN which must match to a precision of ~ 0.01 mag between low and high redshifts (Efstathiou 2025). This is particularly acute for the DES5Y sample which is based on a large photometrically selected SN sample from DES (mainly at redshifts $z \gtrsim 0.2$) but which is supplemented with a small number of nearby SN from various sources at redshifts $\lesssim 0.1$[4]. The DES team responded to this observation using a simulation based investigation to conclude that they saw no reason to alter their analysis of the DES5Y SN compilation (Vincenzi et al. 2025). This issue will not be discussed further in this paper, though it is important to note: (i) that there is no independent check of the Beams with Bias Corrections methodology (Kessler & Scolnic 2017) on which the simulations used in (Vincenzi et al. 2025) are based; (ii) Appendix A of Efstathiou (2025) shows that the DES5Y SN are in tension with the BAO from DESI DR1. As shown in the Appendix to this paper, the tension with DES5Y SN gets worse with DESI DR2.

Given these differences, we ignore the SN data in this paper[5] and concentrate on the consistency between DESI BAO and the CMB. This is an important question because, as noted above, the DESI papers found that the combination of DESI BAO and the CMB favours EvDE at the 3.1σ level: the addition of DES5Y SN, it is argued, merely amplifies a trend in favour of EvDE that is already apparent from the combination of DESI BAO and the CMB.

To investigate this question, Sect. 2 presents a different way of viewing BAO measurements which allow a simple and intuitive test of the ΛCDM cosmology favoured by the CMB. This section addresses whether the BAO measurements from DESI-DR2 strengthen or weaken the evidence for ΛCDM. Section 3 addresses the statistical methodology employed by the DESI collaboration with emphasis on the combination of DESI BAO and the CMB. Our conclusions are summarized in Sect. 4. Appendix A compares the cosmological parameters inferred from DES5Y SN with those from DESI BAO and the CMB.

2 A DIFFERENT ANGLE ON BAO

BAO surveys measure the distance ratios $D_{\rm M}(z)/r_d$ and $D_H(z)/r_d$, where r_d is the sound horizon, $D_{\rm M}$ is the comoving angular diameter distance and $D_H(z)$ is the Hubble distance given by[6]

$$D_{\rm M}(z) = \int_0^z dz' \frac{c}{H(z')}, \tag{2a}$$

$$D_H(z) = \frac{c}{H(z)}, \tag{2b}$$

and $H(z)$ is the Hubble parameter. For a ΛCDM universe with matter density parameter Ω_m, $H(z)$ is given by

$$H(z) = H_0 \left[\Omega_m (1+z)^3 + (1-\Omega_m)\right]^{1/2}. \tag{3}$$

The errors on $D_{\rm M}(z)/r_d$ and $D_H(z)/r_d$ from BAO surveys such as DESI are set by the details of the survey (e.g. redshift, volume, sampling rate, *etc.*) and by aspects of data processing (e.g. BAO reconstruction, estimator *etc.*). However, it is evident from Eqs. 2a and 2b that $D_{\rm M}(z)/r_d$ and $D_H(z)/r_d$ are closely related and hence physics imposes strong constraints on these observables. This becomes clear if we analyse predictions of BAO distance ratios from observations of the CMB. For example, Fig. 12 from Planck Collaboration et al. (2020) shows that in ΛCDM, the CMB

[2] The literature on the DESI results has become very large and is increasing day-by-day, so I will only reference key papers relevant to the discussion presented here. For a survey of recent literature see Giarè et al. (2024).

[3] Note that although we quote the standard deviations from the DESI papers, as discussed in Sect. 3, we disagree with the statistical methodology and the impression that these these numbers are intended to convey.

[4] This has been noticed by a number of other authors: Gialamas et al. (2025); Notari et al. (2025); Huang et al. (2025).

[5] See (Cortês & Liddle 2025) for a statistical argument to justify neglecting the SN.

[6] We assume a spatially flat Universe throughout this paper.

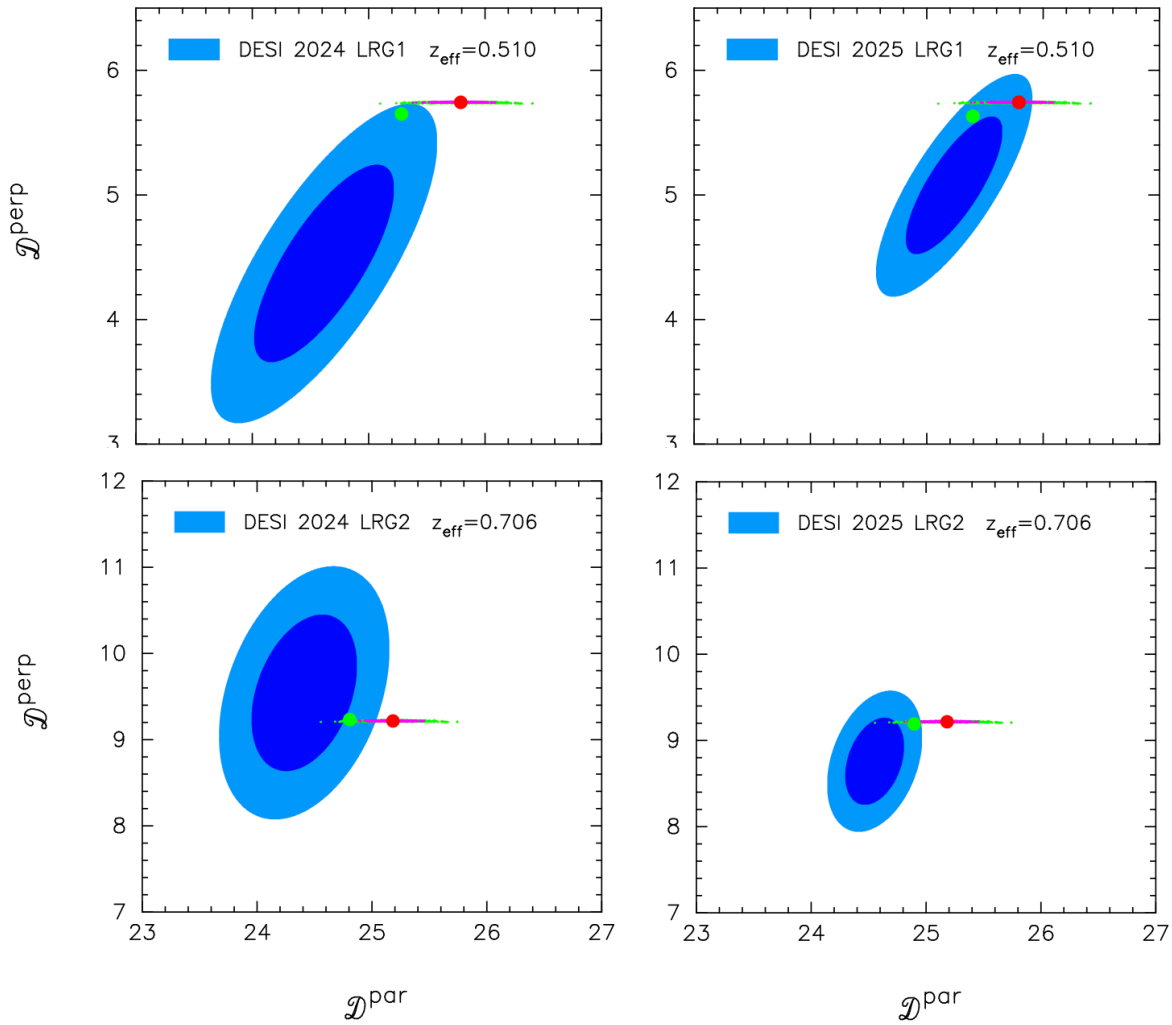

Figure 1. 68% and 95% contours for the rotated BAO parameters $\mathcal{D}^{\rm perp}$ and $\mathcal{D}^{\rm par}$. We show results for the LRG1 and LRG2 surveys for the 2024 DESI DR1 and 2025 DESI DR2 analyses. Samples from the *Planck* base ΛCDM chains are shown by the dots: green for samples from the TT chains and purple for the TTTEEE chains. The spread along the $\mathcal{D}^{\rm par}$direction is determined to high accuracy by the value of the physical matter density parameter $\omega_m = \Omega_m h^2$. The red dots show the best fit values from the *Planck* TTTEEE chains. The green dots show the best fit values for the DESI+$(\theta_*, \omega_b, \omega_{bc})_{\rm CMB}$ fits from DESI-DR1 and DESI-DR2. (Note that ω_{bc} in the DESI papers is denoted ω_m in this paper.)

requires $D_{\rm M}(z)/r_d$ and $D_H(z)/r_d$ to lie on a narrow line of negligible width compared to current BAO constraints.

This behaviour is explained in Sect. 13.5 of Efstathiou & Gratton (2021). In ΛCDM, the parameter combination[7] $\Omega_m h^3$ is very tightly constrained by *Planck* (since this is a good proxy for the acoustic angular scale θ_*). If $\Omega_m h^3$ is fixed, the CMB BAO distance ratios are determined by the physical matter density $\omega_m = \Omega_m h^2$ (with a weak dependence on the baryon density ω_b via the value of the sound horizon r_d, which can be safely neglected in this paper).

It therefore follows that we can define two orthogonal distance ratios $\mathcal{D}^{\rm perp}$ and $\mathcal{D}^{\rm par}$:

$$\mathcal{D}^{\rm par} = (D_H/r_d)\sin\gamma + (D_M/r_d)\cos\gamma, \quad (4a)$$

$$\mathcal{D}^{\rm perp} = (D_H/r_d)\cos\gamma - (D_M/r_d)\sin\gamma, \quad (4b)$$

[7] Where h is the Hubble constant H_0 in units of 100 km s^{-1}Mpc^{-1}.

in which the *Planck* degeneracy line is rotated by an angle γ so that it is horizontal to high accuracy (i.e. parallel to the $\mathcal{D}^{\rm par}$ axis). If the measured value of $\mathcal{D}^{\rm perp}$ lies a long way from the *Planck* line, then this suggests a failure of the ΛCDM cosmology which can be quantified easily.

This is illustrated in Fig. 1 which shows the DESI-DR1 and DESI-DR2 constraints for the Luminous Red Galaxy samples at effective redshifts $z_{\rm eff} = 0.51$ (LRG1) and $z_{\rm eff} = 0.706$ (LRG2). As discussed by the DESI collaboration, it is only LRG1 and LRG2 that show some tension with *Planck* ΛCDM and so we focus on these two samples here. D_M/r_d and D_H/r_d measurements of DESI samples at higher redshift are discussed later in this Section. For obvious reasons, we do not discuss the Bright Galaxy Sample at effective redshift 0.295, since the DESI team present only an isotropised BAO distance ratio, D_V/r_d, for this sample (which has a large error and agrees well with the *Planck* ΛCDM cosmology). One can see evidence for a tension between the DESI-DR1 posterior of $\mathcal{D}^{perp}$ for the LRG1 sample and the *Planck*

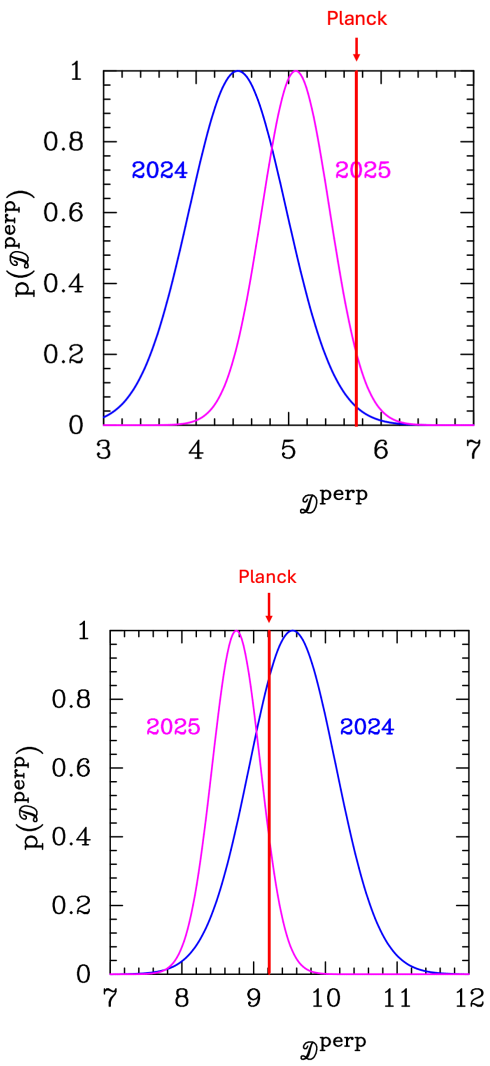

Figure 2. Posterior distributions of $\mathcal{D}^{\rm perp}$ for the DESI DR1 and DR2 LRG1 and LRG2 samples. The *Planck* ΛCDM values (which have negligible error) are shown by the thick red lines. Note the $\sim 2.5\sigma$ tension between the *Planck* value and $\mathcal{D}^{\rm perp}$ measured from the DR1 LRG1 sample, which becomes less significant in DR2.

expectation, but this becomes weaker in DESI-DR2. Since the rotation angles $\gamma(z)$ are fixed by the effective redshift of the sample, the variable $\mathcal{D}^{\rm perp}$ provides a powerful way of testing consistency between *Planck* and BAO under the assumption of ΛCDM because the *Planck* predictions are, to all intents and purposes, a delta function. There is no need to consider nuisance parameters, priors and other complexities. All one has to do is to assess whether there is significant overlap between the DESI posteriors for $\mathcal{D}^{\rm perp}$ and the *Planck* values.

To perform this comparison, we marginalise the DESI constraints over $\mathcal{D}^{\rm par}$ to compute the posterior distrbution of $\mathcal{D}^{\rm perp}$. Define $x = \Delta\mathcal{D}^{\rm perp}$, $y = \Delta\mathcal{D}^{\rm par}$. In the Gaussian approximation

$$P(x,y)dxdy \propto \exp\left(-a_{11}x^2 - a_{22}y^2 - a_{12}xy\right) dxdy,$$

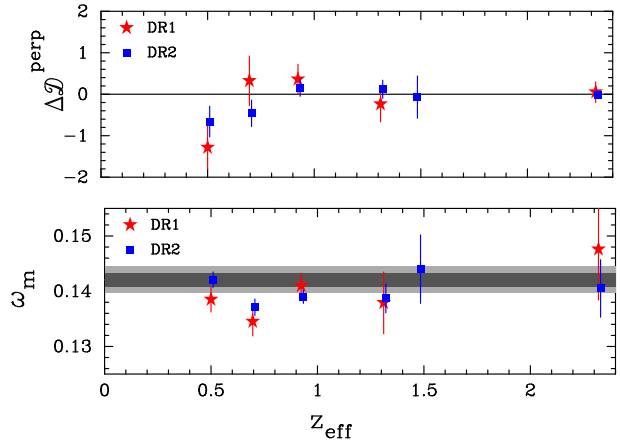

Figure 3. The upper panel shows the residual $\Delta\mathcal{D}^{\rm perp}_{\rm DESI} - \mathcal{D}^{\rm perp}_{\rm Planck}$ as a function of effective redshift for the DESI DR1 and DR2 samples. Note how the DR2 measurements shift closer to the *Planck* values. The lower panel shows the matter density parameter ω_m inferred from the DESI measurements of $\mathcal{D}^{\rm par}$. The horizontal bands show the 1 and 2σ ranges allowed by *Planck* for the base ΛCDM cosmology. As in the upper panel, the DR2 results move closer to the expectations of the *Planck* ΛCDM cosmology.

marginalising over y leads to the distribution

$$P(x)dx \propto \exp\left[\left(-a_{11} + \frac{a_{12}^2}{4a_{22}}\right)x^2\right] dx. \qquad (5)$$

This gives the posterior distribution of $\Delta\mathcal{D}^{\rm perp}$.

The posteriors for $\mathcal{D}^{\rm perp}$ are shown in Fig. 2 for the LRG1 and LRG2 samples. It is clear from Fig. 2 that there is a high degree of overlap with the *Planck* values at both redshifts and furthermore that the 2025 data *are more consistent* with ΛCDM in comparison to the 2024 data. Table 1 lists the rotations to create $\mathcal{D}^{\rm perp}$ and $\mathcal{D}^{\rm par}$ from the DESI measurements together with various statistics including[8] two-tailed p-values for the comparisons between the DESI posteriors for $\mathcal{D}^{\rm perp}$ and the *Planck* values. The residuals of $\Delta\mathcal{D}^{\rm perp} = \mathcal{D}^{\rm perp} - \mathcal{D}^{\rm perp}_{\rm Planck}$ are plotted in the upper panel of Fig. 3 as a function of redshift for all of the DESI samples. This illustrates the spectacular agreement between DESI DR2 and *Planck* ΛCDM over the entire redshift range covered by DESI. As in Fig. 2, the two LRG samples come into better agreement with *Planck* ΛCDM with the improved BAO measurements of DR2. Evidently, there is no evidence from the analysis of $\mathcal{D}^{\rm perp}$ for any significant deviation from the ΛCDM cosmology.

What about the parallel direction? To compute the distribution of $\mathcal{D}^{\rm par}$ conditional on the ΛCDM cosmology, we need to slice the DESI likelihood with $\mathcal{D}^{\rm perp}$ fixed at the *Planck* value (since to a good approximation the slice can be assumed to be infinitely thin). This shifts the mean of

[8] Although I present p-values in Table 1, I will show in Sect. 3 that p-values can be highly misleading when they are applied to 'quantify' more complex comparisons such as the evidence for EvDE.

Table 1. The first column lists the DESI sample and the second column lists the effective redshift. The third column gives the rotation angles γ in radians used to define $\mathcal{D}^{\rm par}$ and $\mathcal{D}^{\rm perp}$. The fourth column gives the values of $\mathcal{D}^{\rm perp}$ computed from the *Planck* TTTEEE ΛCDM chains. These numbers have negligible error. The remaining columns list measurements of $\mathcal{D}^{\rm perp}$ from DESI DR1 and DESI DR2 (mean a posterior values) together with $\pm 1\sigma$ errors. The columns labelled N_σ give the difference between the DESI and *Planck* values of $\mathcal{D}^{\rm perp}$ in units of DESI standard deviation. The columns labeled p-values are computed from N_σ assuming a two-tailed normal distribution.

			Planck	DR1			DR2		
sample	$z_{\rm eff}$	γ	$\mathcal{D}^{\rm perp}$	$\mathcal{D}^{\rm perp}$	N_σ	p-value	$\mathcal{D}^{\rm perp}$	N_σ	p-value
LRG1	0.510	0.816	5.74	4.45 ± 0.52	2.48	0.013	5.08 ± 0.37	1.78	0.075
LRG2	0.706	0.500	9.22	9.54 ± 0.60	-0.53	0.60	8.76 ± 0.34	1.35	0.16
LRG3+ELG1	0.934	0.243	11.76	12.12 ± 0.37	-0.97	0.33	11.92 ± 0.21	-0.76	0.45
ELG2	1.321	0.0274	13.30	13.06 ± 0.43	0.56	0.58	13.42 ± 0.22	-0.54	0.59
QSO	1.484	-0.0177	13.42	-	-	-	13.35 ± 0.51	0.14	0.89
Lyα	2.33	-0.0991	12.46	12.51 ± 0.15	-0.33	0.74	12.448 ± 0.091	0.14	0.89

Table 2. The first two columns are as in Table 1. The third column gives the slope β of Eq. 7 at each redshift necessary to convert measurements of $\mathcal{D}^{\rm par}$ to constraints on ω_m according to the *Planck* ΛCDM cosmology. The columns labelled $\mathcal{D}^{\rm par}$ list the mean a posterior values of $\mathcal{D}^{\rm par}$ from DESI DR1 and DR2 together with $\pm 1\sigma$ errors. The columns labelled ω_m convert the measurements of $\mathcal{D}^{\rm par}$into measurements of ω_m using Eq. 7.

			Planck	DR1		DR2	
sample	$z_{\rm eff}$	β	$\mathcal{D}^{\rm par}$	$\mathcal{D}^{\rm par}$	ω_m	$\mathcal{D}^{\rm par}$	ω_m
LRG1	0.510	0.00836	25.776 ± 0.126	25.35 ± 0.26	0.1385 ± 0.0022	25.62 ± 0.17	0.1421 ± 0.0014
LRG2	0.706	0.00921	25.170 ± 0.115	24.36 ± 0.29	0.1345 ± 0.026	24.63 ± 0.16	0.1371 ± 0.0015
LRG3+ELG1	0.934	0.00934	25.549 ± 0.113	25.44 ± 0.25	0.1410 ± 0.0023	25.22 ± 0.13	0.1390 ± 0.0012
ELG2	1.321	0.00919	28.425 ± 0.115	27.98 ± 0.61	0.1379 ± 0.0056	28.08 ± 0.28	0.1387 ± 0.0026
QSO	1.484	0.00919	30.012 ± 0.115	-	-	30.24 ± 0.67	0.1441 ± 0.0062
Lyα	2.33	0.00975	38.114 ± 0.108	38.69 ± 0.94	0.1476 ± 0.0092	37.95 ± 0.53	0.1405 ± 0.0052

the distribution of $\mathcal{D}^{\rm par}$:

$$P(\mathcal{D}^{\rm par})d\mathcal{D}^{\rm par} \propto \exp\left[-a_{11}\left(\mathcal{D}^{\rm par} - \mathcal{D}^{\rm par}_{\rm DESI} + \frac{a_{12}}{2a_{11}}(\mathcal{D}^{\rm perp}_{\rm Planck} - \mathcal{D}^{\rm perp}_{\rm DESI})\right)\right] d\mathcal{D}^{\rm par}. \quad (6)$$

Significantly, this shift in the mean generally brings the BAO distributions into closer agreement with the *Planck* ΛCDM cosmology. This can be seen in the orientations of the ellipses in Fig. 1, which are tilted towards the *Planck* best fit cosmology. (This tendency is also apparent in Fig. 14 of Adame et al. (2025)).

Results for the parallel statistics are summarized in Table 2. Using the *Planck* ΛCDM TTTEEE chains, the deviation from the *Planck* best-fit value of $\mathcal{D}^{\rm par}$ (listed in the fourth column) is well approximated by the linear relation

$$\omega_m = 0.14205 + \beta(\mathcal{D}^{\rm par} - \mathcal{D}^{\rm par}_{\rm Planck}). \quad (7)$$

Thus, the DESI measurements of $\mathcal{D}^{\rm par}$ (listed in the fifth and seventh columns) can be converted into constraints on the matter density parameter ω_m (listed in the sixth and eighth columns).

The DESI constraints on ω_m are plotted in the lower panel of Fig. 3, together with the *Planck* 1 and 2 σ constraints on ω_m ($\omega_m = 0.14205 \pm 0.00123$). As in the discussion of $\mathcal{D}^{\rm perp}$, the DESI changes from DR1 to DR2 move the points *closer* to the *Planck* value. There is mild tension in the value of ω_m inferred from the LRG2 sample: for DR2, the value of ω_m is about 2.6σ lower than expected from *Planck* (adding the errors from both measurements in quadrature). Averaging over all redshifts, the best fit values of ω_m are 0.1384 ± 0.0015 from DR1 and 0.13947 ± 0.00073 from DR2 differing from the *Planck* value by ~ 1.9 and 1.8σ respectively. For reference, the recent results from the Atacama Cosmology Telescope (ACT) (Louis et al. 2025) for the P-ACT combination (TTTEEE *Planck* power spectra at $\ell < 1000$ and ACT spectra at higher multipoles) give $\omega_m = 0.1425 \pm 0.0012$, i.e. very close to the *Planck* result.

In summary, the analysis of this Section presents a different way of viewing BAO that makes it easy to assess whether the measurements are compatible with ΛCDM cosmology. In addition, we have shown that DESI-DR2 measurements are more consistent with the *Planck* ΛCDM cosmology than DESI-DR1, despite the large increase in statistical power of DESI-DR2 over DESI-DR1. This conclusion differs from that presented in DESI-DR2 who conclude that the consistency between *Planck* ΛCDM and DESI BAO gets marginally worse between DR1 and DR2 (1.9σ discrepancy for DR1 rising to 2.3σ for DR2). The DESI test is based on the constraints on the two parameters Ω_m and $H_0 r_d$. Neither of these parameters are as well constrained by the CMB as $\mathcal{D}^{\rm perp}$ and ω_m and so the DESI test is not as precise as that presented here. It is difficult to argue against the re-

sults shown in Figs 2 and 3 that DESI DR2 BAO come into better consistency with *Planck* ΛCDM.

Although ΛCDM appears to be a good description of both the CMB and the BAO measurements, the DESI collaboration argue that the situation changes with the introduction of EvDE. Including the additional parameters w_0 and w_a from Eq. 1, they claim to find a solution that 'is preferred over ΛCDM at 3.1σ for the combination of DESI BAO and CMB data'. The veracity of this statement is the subject of the next Section.

3 COMBINING BAO AND THE CMB: ANOTHER ROTATION

In this Section, I will follow the DESI collaboration and use a compressed CMB likelihood consisting of three parameters (θ_*, ω_b, ω_m, see Eqs A1 and A2 of DESI-DR2). I will denote this likelihood QCMB. The simplified CMB likelihood is perfectly adequate for our purposes and is insensitive to physical processess that have nothing to do with EvDE that can lead, via the late-time integrated Sachs-Wolfe (ISW) effect (Sachs & Wolfe 1967; Rees & Sciama 1968), to small shifts that can be mistaken for EvDE (though always at low statistical significance). Analysis of such effects will be deferred to another paper.

The left hand panel of Fig. 4 shows the constraints from DESI-DR2 if w_0 and w_a are allowed to vary as additional parameters to those of ΛCDM[9]. Following DESI-DR2 we denote these models as $w0wa$CDM. Adding the QCMB likelihood leads to the red contours in Fig. 4. These contours agree well with those in Fig. 14 of DESI-DR2 (which are actually close to those using the full `CamSpec` TTTEEE *Planck* likelihood). Now let us follow the interpretation given in DESI-DR2. The DESI team calculate $\Delta\chi^2_{\rm MAP}$, which is the difference in χ^2 at the maximum a posteriori likelihood of the w0waCDM model and the maximum a posterior likelihood for ΛCDM. In this case, $\Delta\chi^2_{\rm MAP} = -8.0$. Thus adding two additional parameters leads to improved fits to the data. Assuming a χ^2 distribution with two degrees of freedom, the $\Delta\chi^2_{\rm MAP}$ gives a p-value of 0.0183. This p-value is then converted into 'standard deviations' by matching to the two-tailed p-value of a normal distribution. In this case, the result is summarized as a 2.4σ preference for EvDE. The impression given by these numbers is that there is a preference for w0waCDM and the odds are stacked against ΛCDM by about 55:1. Is this a reasonable conclusion?

One can see from Fig. 4 that the red contours are quite narrow and oriented towards the ΛCDM point $w_0 = -1$, $w_a = 0$. (Note that the main effect of the more accurate BAO measurements from DESI-DR2 is to make the contours narrower perpendicular to the main degeneracy direction). It is clear from this Figure that w_0 and w_a are highly correlated. The green dashed line in the left hand panel of Fig. 4 is computed as follows. Define $w_{\rm piv}$ to be the value of the equation-of-state parameter at a pivot redshift, $z_{\rm piv}$:

$$w_{\rm piv} = w_0 + w_a \left(\frac{z_{\rm piv}}{1+z_{\rm piv}}\right). \tag{8}$$

Now fix $w_{\rm piv} = -1$ at a redshift at which $w(z)$ is determined accurately by the data, say $z_{\rm piv} = 0.5$. In this case,

$$w_0 = -1 - w_a \left(\frac{z_{\rm piv}}{1+z_{\rm piv}}\right), \tag{9}$$

which is plotted as the green dashed line in Fig. 4[10]. Evidently, if we choose to reparameterize (w_0, w_a) in terms of $w_{\rm piv} \equiv w(z_{\rm piv})$, the parameters $w_{\rm piv}$ and w_a will decorrelate. This is illustrated in the right hand panel of Fig. 4. With this rotation, the maginalised EvDE parameters are:

$$w_{\rm piv} = -1.08 \pm 0.10,\ \ w_a = -2.81 \pm 1.38,\ \ \text{DESI}, \tag{10a}$$

$$w_{\rm piv} = -0.996 \pm 0.046,\ \ w_a = -1.78 \pm 0.79,\ \ \text{DESI} + \text{QCMB}. \tag{10b}$$

For both data combinations, $w_{\rm piv}$ is consistent with the ΛCDM value of $w = -1$ and it is accurately determined by the data. The $\Delta\chi^2_{\rm MAP}$ is of course unchanged and so according to the interpretation of the DESI collaboration the odds in favour of EvDE remain at about 55:1 and the fact that $w(z)$ agrees with the ΛCDM value at a redshift where it is well determined by the data is a coincidence. The peculiarity of this conclusion has been pointed out by Cortês & Liddle (2025).

The interpretation becomes even more peculiar if we fix $w_{\rm piv}$ = -1 and test a model of EvDE which has only one parameter w_a. In this case, $\Delta\chi^2_{\rm MAP}$ does not change because the maximum a posterior value of w_a lies accurately along the degeneracy direction of Eq. 9. However, this model has only one parameter and so the odds in its favour increase to $212:1$ (increasing the preference for EvDE from 2.4σ to 2.8σ). So is this model more likely than the w_0, w_a parameterization? Intuitively, the one parameter model seems more contrived *but crucially there is no measure of contrivedness in the DESI statistical methodology.*

The Bayesian solution to this type of problem is well known. One computes the Evidence (the probability of the data D given the model M):

$$E(M) = \int d\boldsymbol{\theta} P(D|\boldsymbol{\theta}M)\pi(\boldsymbol{\theta}|M), \tag{11}$$

where $\pi(\boldsymbol{\theta}|M)$ is the prior distribution of model parameters $\boldsymbol{\theta}$ and $P(D|\boldsymbol{\theta}M)$ is the likelihood of the parameters under model M. If we have two models, M_1 and M_2, the Bayes factor $B_{12} = E(M_1)/E(M_2)$ provides a measure with which to discriminate between the models. Critically, the Evidence requires specification of the prior distribution $\pi(\boldsymbol{\theta}|M)$. I have previously written about the limitations of Bayesian Evidence applied to cosmology (Efstathiou 2008). This is not because Evidence is the wrong thing to calculate, but rather

[9] We use the `MULTINEST` nested sampler (Feroz et al. 2009, 2011) to produce parameter chains in this paper. The choices of priors are as described in Efstathiou (2025).

[10] The dashed line defined by Eq. 9 is quite close to the CMB geometric degeneracy direction in which models with w_0, w_a have the same angular diameter distance to the last scattering surface. It is this unfortunate alignment of the degeneracy directions that make it difficult to constrain EvDE using BAO and the CMB.

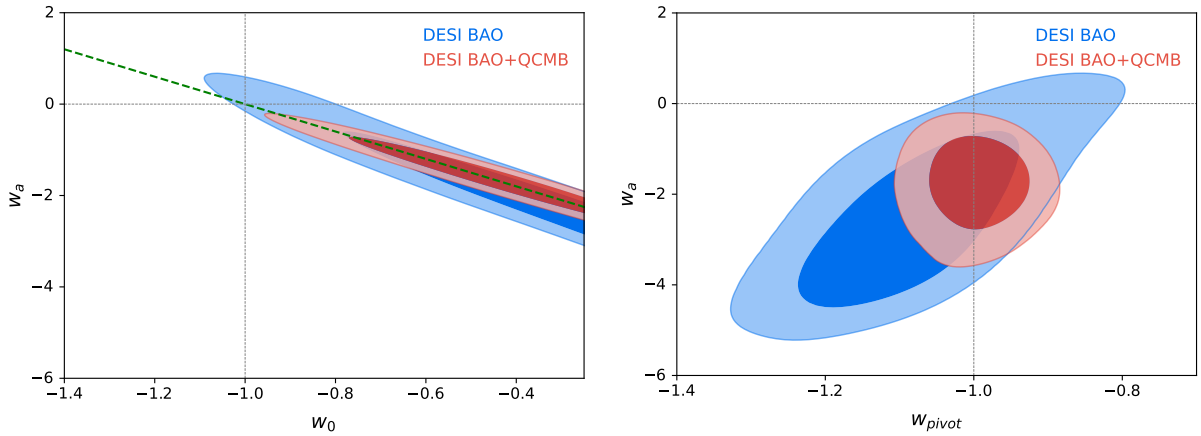

Figure 4. The left hand panel shows 68% and 95% contours for the marginalized posterior parameters in the $w_0 - w_a$, $w_0 - \Omega_m$ and $w_a - \Omega_m$ planes for the Pantheon+ (red) and DES5Y (blue) SN compilations. The dashed lines show the values for the best fit *Planck* ΛCDM cosmology. The green dashed line shows the relation of Eq. 9 determined by fixing $w_{\rm piv} = w(z_{\rm piv}) = -1$ at a pivot redshift $z_{\rm piv} = 0.5$. The right hand panel shows the constraints on $w_{\rm piv}$ and w_a, illustrating the tight constraints on $w_{\rm piv}$ and the decorrelation of $w_{\rm piv}$ from w_a.

that in cosmology we often have no guidance on how to choose priors. Hence there is no objective way of computing Bayes factors that everybody can agree on. The ideal situation in Bayesian statistics is for the data to overwhelm the priors. This happens in the *Planck* analysis of ΛCDM for parameters such as ω_b, ω_c etc. But the situation is very different if the ΛCDM model is extended, for example, to include curvature Ω_K. In this case, the CMB displays a strong geometric degeneracy and so the interpretation of CMB data alone becomes very sensitive to priors. This is an especially difficult problem because unlike parameters such as ω_b and ω_c, there are good theoretical reasons for why there may be an attractor driving Ω_K to a particular value. Thus, in inflationary cosmology $\Omega_K = 0$ is a special case. Fortunately the geometrical degeneracy is broken decisively by other data, especially BAO, leading to the strong constraint $\Omega_K = 0.0004 \pm 0.0018$, consistent with inflationary cosmology (for further discussion of these issues see Efstathiou & Gratton 2020).

As with Ω_K, a strong geometrical degeneracy re-emerges if the ΛCDM cosmology is extended to include the dark energy parameters w_0 and w_a. The CMB constraints on these parameters then stratify along lines of constant angular diameter distance to recombination with only a weak dependence coming from the ISW effect to break the degeneracy (see e.g. Fig. 30 of Planck Collaboration et al. 2020). However, unlike the case of Ω_K, BAO constraints follow almost the same degeneracy direction as the CMB (see Fig. 4) and so do not decisively break the geometrical degeneracy. This means that the combination of CMB+BAO is mired in the swampland of $\sim 2-3\sigma$ statistics, where the interpretation is strongly dependent on choices of priors (the bane of cosmological inference).

How do we choose priors in the case of EvDE? This is even more difficult than choosing a prior for Ω_K. We have no theoretical understanding of the cosmological constant problem (Weinberg 1989) apart from possible anthropic explanations[11] (Weinberg 1987; Efstathiou 1995). In fact, prior to the discovery of dark energy (Riess et al. 1998; Perlmutter et al. 1999), the prior $\Lambda = 0$ favoured by the majority of theorists would have been wide of the mark. The case of EvDE poses even more difficulties than Λ. To display interesting dynamical behaviour at late times, a scalar field model of EvDE must involve a very small mass of $\sim 10^{-32}$eV. This requires some sort of shift symmetry to protect the small mass from radiative corrections. In addition, to produce $w_{\rm piv}$ close to -1, as demanded by the data (Eq. 9), requires fine tuning of the potential. Thus although models can be constructed that map onto the region of w_0, w_a space allowed by the data, (Shlivko & Steinhardt 2024; Wolf et al. 2025a,b; Shlivko et al. 2025), the parameters involve unexplained fine-tunings. It therefore seems reasonable to this author that models of EvDE should be given a *substantial* penalty compared to ΛCDM. How big a penalty is entirely subjective[12], but requiring odds of order $10^6 : 1$ or more (i.e. about the threshold of 5σ commonly applied in particle physics) would seem reasonable before claiming evidence for new physics.

4 CONCLUSIONS

The first part of this paper should be uncontroversial. It presents a different way of looking at the DESI BAO data by constructing orthogonal linear combinations of D_H/r_d and D_M/r_d, $\mathcal{D}^{\rm perp}$and $\mathcal{D}^{\rm par}$, designed to simplify tests of the *Planck* ΛCDM cosmology. The analysis is not merely a trivial rotation, however, because in comparing with ΛCDM we can impose constraints on the DESI measurements to account for regions of parameter space that are inaccessible to a ΛCDM cosmology.

[11] Which this author believes are ill-posed in the context of inflationary cosmology.
[12] As is clear from the arguments presented by Brandenberger (2025).

The results for $\mathcal{D}^{\rm perp}$ plotted in the upper panel of Fig. 2 for the LRG1 and LRG2 samples (which in DR1 showed the strongest discrepancy with *Planck* ΛCDM) demonstrate unambiguously that DESI DR2 measurements move closer towards the expectations of *Planck* ΛCDM. In addition, the changes in DR2 bring the BAO measurements for LRG1 and LRG2 into closer agreement with the earlier SDSS/BOSS measurements summarized by Alam et al. (2017). The improvement in the consistency in $\mathcal{D}^{\rm perp}$ between DESI BAO and *Planck* ΛCDM extends over the entire redshift range of the DESI measurements. We find similar consistency for the orthogonal statistic $\mathcal{D}^{\rm par}$ as shown in the lower panel of Fig. 2. Despite the increase in statistical power of DESI DR2, the measurements move closer to *Planck* ΛCDM *with no evidence to support EvDE*. This is a triumph for experiment and theory, for which the DESI collaboration deserves enormous credit.

I suspect that the second part of the paper will be considered more controversial, though it is based on well-worn arguments in Bayesian statistics (see e.g. Jaynes 2003; MacKay 2003). The DESI collaboration argue that if DESI BAO are combined with *Planck* CMB, EvDE is preferred over ΛCDM at the 3.1σ level with the clear implication that the odds in favour of EvDE are about 500:1. But probability represents a degree of belief and is necessarily subjective. In physics, and especially in cosmology, there are rarely symmetry principles or other considerations to objectively fix priors. Hence there is no objective measure of the odds in favour of EvDE.

To believe that the data points to EvDE, one needs to:

(i) believe that any model in the w_0, w_a plane[13] has the same prior probability as Λ;
(ii) believe that out of all possible models for EvDE, those favoured by the data have $w_{\rm piv}$ at $z_{\rm piv} = 0.5$ very close to -1 (Eq. 8) and that it is a coincidence that the density of dark energy happens to peak at a redshift at which the equation-of-state is accurately determined by the data;
(iii) believe that the heuristic $\Delta\chi^2_{\rm MAP}$ statistic[14] accurately accounts for overfitting of the data and gives a measure of the odds against ΛCDM;
(iv) disregard the fact that with the very substantial increase in statistical power of DESI BAO from DR1 to DR2 there is almost no change in the 'significance' levels quoted by the DESI collaborations in favour of EvDE. (Noting that in this paper we find that DR2 gives better consistency with ΛCDM than DR1, particularly for the $\mathcal{D}^{\rm perp}$ statistic.);
(v) discount the fact that the inclusion of powerful new CMB data from ACT (Louis et al. 2025) in place of, or in addition to, *Planck* does not significantly strengthen the evidence for EvDE and that some ACT+*Planck* data combinations actually weaken the evidence for EvDE (Garcia-Quintero et al. 2025).

[13] Apart from imposing a prior $w_0 + w_a < 0$ to ensure matter domination at high redshift.
[14] DESI-DR1 and DESI-DR2 also quote changes in the Deviance Information Criterion ΔDIC, but this statistic is based on the sampling chains with uniform priors in w_0, w_a. ΔDIC adds nothing new and is in fact well approximated by $\Delta\chi^2_{\rm MAP} = \Delta{\rm DIC} - 4$. Lodha et al. (2025) quote Bayes factors for some models, but again assuming the same priors as those used in the sampling chains.

A quantity such as $\Delta\chi^2_{\rm MAP}$ cannot, and should not, be used to imply a probability. Degrees of belief are subjective quantities and so there will be differences of opinion unless data so overwhelm reasonable choices of priors that a consensus emerges.

What about the SN? As noted in the introduction, The impact of adding SN to DESI and BAO is strongly dependent on which SN compilation is used. Until the reasons for these differences are understood, it is dangerous to place much faith in the SN (see also Cortês & Liddle 2025) and highly misleading to present results for one SN compilation while ignoring the others (see e.g. Shajib & Frieman 2025). I have previously argued that there may be a systematic mismatch in the photometry of nearby ($z \lesssim 0.1$) SN and those at higher redshift that drives cosmological parameters inferred from the DES5Y catalogue into regions of parameter space that are strongly disfavoured by other data (Efstathiou 2025). Appendix A provides an update and shows that the tension between parameter constraints from DES5Y SN and those determined from DESI BAO and the CMB gets worse from DR1 to DR2. This should raise serious concerns about whether it is reasonable to combine DES5Y SN with BAO and the CMB.

5 ACKNOWLEDGEMENTS

I thank the Leverhulme Foundation for the award of a Leverhulme Emeritus Fellowship.

DATA AVAILABILITY

No new data were generated or analysed in support of this research.

APPENDIX A: COMPARISON OF COSMOLOGICAL PARAMETER CONSTRAINS FROM DES5Y SN COMPARED TO DESI DR2 BAO AND QCMB

Figure A1 compares cosmological constraints from the DES5Y SN catalogue in the space of $w_{\rm piv}$. w_a and Ω_m. As discussed in Efstathiou (2025) the DES5Y contours are skewed to high values of Ω_m that are disfavoured by o the other data. In the central panel there is a clear separation between $w_{\rm piv}$ between the DES5Y SN and the constraints from DESI BAO, which favour $w_{\rm piv}$ close to -1 to high accuracy. One can clearly see how the DES5Y SN data drag the rest of the data away from the cosmological constant point. For DESI BAO + DES5Y SN + QCMB, we find $\Delta\chi^2_{\rm MAP} = 17.1$ relative to ΛCDM. Following the statistical methodology of the DESI collaboration, this gives a p-value of 0.0001297 corresponding to a 3.8σ 'preference' for EvDE over ΛCDM.

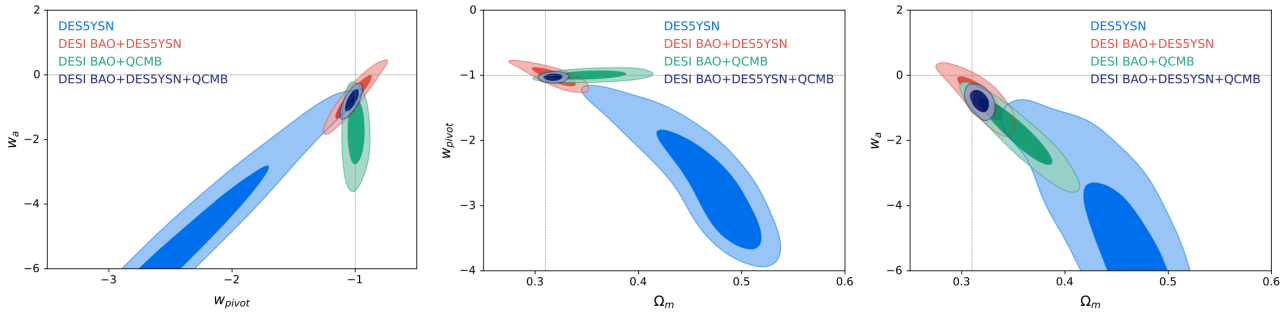

Figure A1. 68% and 95% contours for the marginalized posterior parameters in the $w_{\rm piv} - w_a$, $w_{\rm piv} - \Omega_m$ and $w_a - \Omega_m$ planes for DES5Y (blue) SN compilations. The remaining contours show DES5Y combined with QCMB (green), DESI BAO combined with DES5YSN (red), and DESI BAO combined with DES6YSN and QCMB (dark blue). The dashed lines show the values for the best fit *Planck* ΛCDM cosmology.

REFERENCES

Adame A. G., et al., 2025, J. Cosmology Astropart. Phys., 2025, 012
Alam S., et al., 2017, MNRAS, 470, 2617
Brandenberger R., 2025, arXiv e-prints, p. arXiv:2503.17659
Chevallier M., Polarski D., 2001, International Journal of Modern Physics D, 10, 213
Cole S., et al., 2005, MNRAS, 362, 505
Cortês M., Liddle A. R., 2025, arXiv e-prints, p. arXiv:2504.15336
DES Collaboration et al., 2024, arXiv e-prints, p. arXiv:2401.02929
DESI Collaboration et al., 2024, arXiv e-prints, p. arXiv:2404.03002
DESI Collaboration et al., 2025, arXiv e-prints, p. arXiv:2503.14738
Efstathiou G., 1995, MNRAS, 274, L73
Efstathiou G., 2008, MNRAS, 388, 1314
Efstathiou G., 2025, MNRAS, 538, 875
Efstathiou G., Gratton S., 2020, MNRAS, 496, L91
Efstathiou G., Gratton S., 2021, The Open Journal of Astrophysics, 4, 8
Eisenstein D. J., et al., 2005, ApJ, 633, 560
Feroz F., Hobson M. P., Bridges M., 2009, MNRAS, 398, 1601
Feroz F., Hobson M. P., Bridges M., 2011, MultiNest: Efficient and Robust Bayesian Inference (ascl:1109.006)
Garcia-Quintero C., et al., 2025, arXiv e-prints, p. arXiv:2504.18464
Gialamas I. D., Hütsi G., Kannike K., Racioppi A., Raidal M., Vasar M., Veermäe H., 2025, Phys. Rev. D, 111, 043540
Giarè W., Najafi M., Pan S., Di Valentino E., Firouzjaee J. T., 2024, J. Cosmology Astropart. Phys., 2024, 035
Huang L., Cai R.-G., Wang S.-J., 2025, arXiv e-prints, p. arXiv:2502.04212
Jaynes E. T., 2003, Probability theory: The logic of science. Cambridge University Press, Cambridge
Kessler R., Scolnic D., 2017, ApJ, 836, 56
Linder E. V., 2003, Phys. Rev. Lett., 90, 091301
Lodha K., et al., 2025, arXiv e-prints, p. arXiv:2503.14743
Louis T., et al., 2025, arXiv e-prints, p. arXiv:2503.14452
MacKay D. J. C., 2003, Information Theory, Inference, and Learning Algorithms. Copyright Cambridge University Press
Notari A., Redi M., Tesi A., 2025, J. Cosmology Astropart. Phys., 2025, 048
Perlmutter S., et al., 1999, ApJ, 517, 565
Planck Collaboration et al., 2020, A&A, 641, A6
Poulin V., Smith T. L., Karwal T., 2023, Physics of the Dark Universe, 42, 101348
Rees M. J., Sciama D. W., 1968, Nature, 217, 511
Riess A. G., et al., 1998, AJ, 116, 1009
Rubin D., et al., 2023, arXiv e-prints, p. arXiv:2311.12098
Sachs R. K., Wolfe A. M., 1967, ApJ, 147, 73
Sánchez B. O., et al., 2024, arXiv e-prints, p. arXiv:2406.05046
Scolnic D., et al., 2022, ApJ, 938, 113
Shajib A. J., Frieman J. A., 2025, arXiv e-prints, p. arXiv:2502.06929
Shlivko D., Steinhardt P. J., 2024, Physics Letters B, 855, 138826
Shlivko D., Steinhardt P. J., Steinhardt C. L., 2025, arXiv e-prints, p. arXiv:2504.02028
Vincenzi M., et al., 2024, arXiv e-prints, p. arXiv:2401.02945
Vincenzi M., et al., 2025, arXiv e-prints, p. arXiv:2501.06664
Weinberg S., 1987, Phys. Rev. Lett., 59, 2607
Weinberg S., 1989, Reviews of Modern Physics, 61, 1
Weinberg D. H., Mortonson M. J., Eisenstein D. J., Hirata C., Riess A. G., Rozo E., 2013, Phys. Rep., 530, 87
Wolf W. J., García-García C., Ferreira P. G., 2025a, arXiv e-prints, p. arXiv:2502.04929
Wolf W. J., García-García C., Anton T., Ferreira P. G., 2025b, arXiv e-prints, p. arXiv:2504.07679